

---

**Review**

---

# Double Beta Decay Experiments: Recent Achievements and Future Prospects

---

Alexander Barabash

## Special Issue

Recent Advances in Double Beta Decay Investigations: In Honor of Prof. Sabin Stoica at His 70th Anniversary

Edited by

Prof. Dr. Mihai Horoi, Prof. Dr. Hiro Ejiri and Dr. Andrei Neacsu

Review

# Double Beta Decay Experiments: Recent Achievements and Future Prospects

Alexander Barabash 

National Research Centre “Kurchatov Institute”, Kurchatov Complex of Theoretical and Experimental Physics, B. Cheremushkinskaya 25, 117218 Moscow, Russia; barabash@itep.ru; Tel.: +7-916-933-9350

**Abstract:** The results of experiments on the search for and study of double beta decay processes obtained over the past 5 years (from 2018 to April 2023) are discussed. The results of the search for neutrinoless double beta decay are presented, in which a sensitivity of  $T_{1/2} \sim 2 \times 10^{24}$ – $2 \times 10^{26}$  years (90% C.L.) has been achieved. The present conservative upper limit on effective Majorana neutrino mass  $\langle m_\nu \rangle$  was established from these experiments as 0.16 eV (90% C.L.). The results of experiments on recording and studying the processes of two-neutrino double beta decay in various nuclei (transitions to both the ground and excited states of daughter nuclei) are discussed too. The results of experiments on the search for majoron are also given. Possible progress in this field in the future is discussed.

**Keywords:** double beta decay; neutrino mass; majoron

## 1. Introduction

The search for neutrinoless double beta decay ( $0\nu\beta\beta$ ) is one of the most urgent topics in nuclear physics and elementary particle physics. The detection of this process will automatically lead to two fundamental discoveries: (1) a violation of the lepton number ( $L$ ) conservation will be established (which is a necessary condition for leptogenesis, a leading explanation of why the universe is matter dominated [1]), and (2) it will be established that neutrinos are Majorana particles, meaning that neutrinos are the same as antineutrinos [2]. In addition, it could provide information on such fundamental issues as the neutrino eigenstate masses, the type of ordering of neutrino masses, and may be even CP violation in the lepton sector (see discussions in [3–6]). The detection of a process with the emission of a majoron will lead to the discovery of a new elementary particle, the majoron, which is one of the candidates for dark matter. All this, in turn, will lead to the most important consequences in physics and astrophysics. The study of various isotopes and types of decay will provide information on the mechanism of  $0\nu\beta\beta$  decay. The measurement and study of two-neutrino double beta decay ( $2\nu\beta\beta$ ) is also of great interest. Obtaining experimental information about the values of nuclear matrix elements (NME( $2\nu$ )) makes it possible to improve NME calculations for both two-neutrino and neutrinoless decays. A detailed study of the spectrum shape makes it possible to search for processes outside the framework of the standard model: the existence of bosonic neutrinos [7], the Lorentz invariance violation [8,9], the neutrino self-interactions [10], the existence of sterile neutrinos [11], and the search for right-handed neutrinos [12].

This review presents the results of experiments performed from the beginning of 2018 to April 2023. The results of earlier experiments can be found in [13–18]. The theoretical aspects of  $\beta\beta$  decay are well presented in recent reviews [4,18–20].

## 2. Results of Recent Experiments

Tables 1–7 present all significant results on the search for different types of  $\beta\beta$  processes obtained from the beginning of 2018 to the present (April 2023).



**Citation:** Barabash, A. Double Beta Decay Experiments: Recent Achievements and Future Prospects. *Universe* **2023**, *9*, 290. <https://doi.org/10.3390/universe9060290>

Academic Editor: Marco Selvi

Received: 27 April 2023

Revised: 22 May 2023

Accepted: 13 June 2023

Published: 15 June 2023



**Copyright:** © 2023 by the authors. Licensee MDPI, Basel, Switzerland. This article is an open access article distributed under the terms and conditions of the Creative Commons Attribution (CC BY) license (<https://creativecommons.org/licenses/by/4.0/>).

## 2.1. Results for $0\nu\beta\beta$ Decay

Neutrinoless double beta decay is a process in which the nucleus ( $A, Z$ ) is transformed into the nucleus ( $A, Z + 2$ ) with the simultaneous emission of two electrons:

$$(A, Z) \rightarrow (A, Z + 2) + 2e^- . \quad (1)$$

Since the energy of the recoil nucleus in this process is negligible, the sum of the kinetic energies of two electrons must equal the energy released in the decay for this transition ( $Q_{\beta\beta}$ ). Neutrinoless double beta decay can occur through various mechanisms. Here, we will consider the most popular scheme with light neutrinos. In this case, the decay probability is written as follows [19,21]:

$$[T_{1/2}(0\nu)]^{-1} = G_{0\nu} g_A^4 | M_{0\nu} |^2 \left| \frac{\langle m_\nu \rangle}{m_e} \right|^2 , \quad (2)$$

where  $G_{0\nu}$  is the phase space factor, which contains the kinematic information about the final state particles, and is exactly calculable to the precision of the input parameters [21,22],  $g_A$  is the axial-vector coupling constant,  $| M_{0\nu} |^2$  is the nuclear matrix element,  $m_e$  is the mass of the electron, and  $\langle m_\nu \rangle$  is the effective Majorana mass of the electron neutrino, which is defined as  $\langle m_\nu \rangle = | \sum_i U_{ei}^2 m_i |$ , where  $m_i$  are the neutrino mass eigenstates and  $U_{ei}$  are the elements of the neutrino mixing Pontecorvo–Maki–Nakagawa–Sakata (PMNS) matrix  $U$ .

Table 1 presents the results of experiments on the search for  $0\nu\beta\beta$  decay, as well as the main parameters of the installations used. It can be seen that eight different isotopes were studied using completely different techniques and detectors. The measurement statistics are also different, from 0.12 kg·yr in the CANDLES-III [23] experiment to 970 kg·yr in the KamLAND-Zen [24] experiment. An important parameter is the energy resolution of the detectors (FWHM) in the region of  $Q_{\beta\beta}$ . The best energy resolution was achieved in the Majorana Demonstrator [25] experiment with HPGe detectors (2.52 keV), while the worst was found in the NEMO-3 [26] and KamLAND-Zen [24] experiments ( $\sim 250$  keV). One of the most important parameters of such installations is the background index (BI) in the energy range of  $0\nu\beta\beta$  decay and the background index multiplied by the energy resolution (BI·FWHM). The lowest background index was obtained in the KamLAND-Zen [24] experiment ( $\sim 7 \times 10^{-5}$  c/keV·kg·yr), but the best BI·FWHM value (which is much more important) was obtained in the GERDA [27] experiment ( $\sim 1.8 \times 10^{-3}$  c/kg·yr).

The limits presented in Table 1 are the best to date and define the state of the research in  $0\nu\beta\beta$  decay. In the experiments with the best sensitivity (KamLAND-Zen [24] and GERDA [27]), a limit on the half-life of  $\sim 2 \times 10^{26}$  years was achieved; in three experiments [25,28,29], limits of  $\sim (2-8) \times 10^{25}$  years were attained; and in other three experiments [30–32], limits of  $\sim (2-4) \times 10^{24}$  years were obtained (all limits at 90% C.L.). The limits on  $\langle m_\nu \rangle$  are given in the seventh column of Table 1 (these are the values given by the authors in the relevant publications). It can be seen that in all cases, we are dealing with a fairly wide range of values. This is due to uncertainties in the NME calculations. Still, more conservative values seem to be more realistic (closer to the right boundary of the interval), and it is on them that one should reply when planning new experiments. From the obtained results, we can conservatively conclude that the current limit on  $\langle m_\nu \rangle$  is  $\sim 0.16$  eV (90% C.L.). The current state of the problem of NME calculations can be found in [18–20,33,34].

Only three experiments from Table 1 are still active today: these are KamLAND-Zen, CUORE, and CANDLES-III. It can be expected that in a few years, new, several times more stringent limits on  $T_{1/2}$  for  $^{136}\text{Xe}$ ,  $^{130}\text{Te}$ , and  $^{48}\text{Ca}$  will be obtained. In addition, in 2023, LEGEND-200 started the data taking (see Section 3).

Using the data of oscillatory experiments, one can obtain predictions for possible values of  $\langle m_\nu \rangle$ . Usually, a so-called “lobster” plot is constructed, which shows the possible values of  $\langle m_\nu \rangle$ , depending on the type of ordering and the mass of the lightest neutrino  $m_0$ , which is unknown. The cosmological constraints on  $\Sigma m_\nu$  are used to limit the possible values of  $m_0$ . The PLANCK collaboration gives a limit of  $\Sigma m_\nu < 0.12$  eV [35], using the CMB

data with different large-scale structure observations. This leads to a limitation on  $m_0 < 30$  and  $< 16$  meV for normal and inverted ordering, respectively. In Figure 1, predictions on the effective Majorana neutrino mass are plotted as a function of the lightest neutrino mass  $m_0$ . The  $2\sigma$  and  $3\sigma$  values of neutrino oscillation parameters are taken into account [36]. The gray area indicates the sensitivity region of the KamLAND-Zen experiment on  $0\nu\beta\beta$  decay (36–156 meV) [24]. It can be seen that at the maximum NME values for  $^{136}\text{Xe}$ , the KamLAND-Zen experiment is sensitive to the region with the inverse neutrino mass ordering. However, at low values of NME (which, apparently, is more likely), the sensitivity still does not reach this region. Additionally, the main goal of the future experiments is to test the scheme with the inverted ordering of neutrino masses (see Section 3).

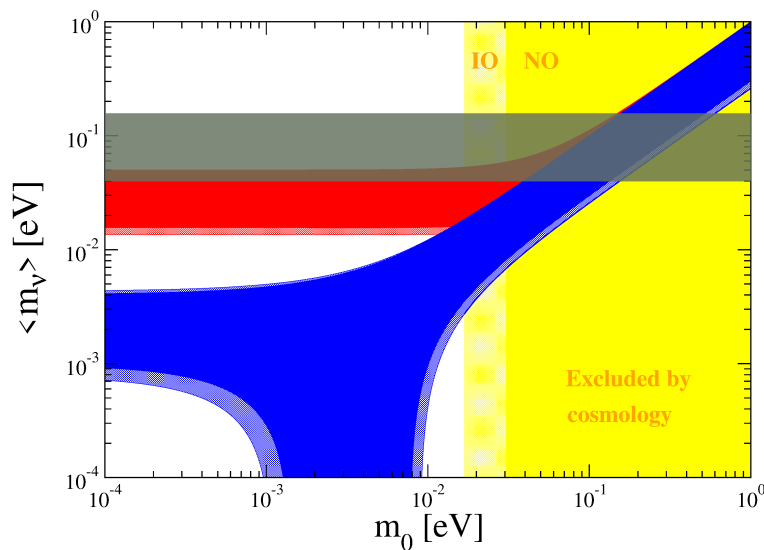


**Figure 1.** Predictions on  $\langle m_\nu \rangle$  from neutrino oscillations versus the lightest neutrino mass,  $m_0$ , in the two cases of the normal (NO, the on-line blue region) and inverted (IO, the on-line red region) ordering of the neutrinos' masses. The  $2\sigma$  and  $3\sigma$  values of neutrino oscillation parameters are considered [36]. The  $m_0$  region that is disfavored by cosmological data ( $\Sigma m_\nu < 0.12$  eV) is presented in (on-line) yellow ( $> 30$  meV for NO and  $> 16$  meV for IO). The gray area indicates the sensitivity region of the KamLAND-Zen experiment on  $0\nu\beta\beta$  decay (36–156 meV) [24].

**Table 1.** Limits for  $0\nu\beta\beta$  decay in experiments conducted from 2018 to April 2023. Limits on  $\langle m_\nu \rangle$  are given as intended by the authors of the respective publications.  $Q_{\beta\beta}$  is energy of  $0\nu\beta\beta$  transition;  $M$  is mass of the investigated material (in parentheses, the mass of the investigated isotope is used);  $t$  is measurement time; FWHM (full width at half maximum) is energy resolution at  $Q_{\beta\beta}$ ; BI is background index; LTB is low-temperature bolometer. <sup>(a)</sup> For Module-II it is  $8.7 \times 10^{-3}$ . <sup>(b)</sup> This is the mass of liquid scintillator in the fiducial volume. <sup>(c)</sup> Obtained using 21 of 93  $\text{CaF}_2$  crystals.

Nucleus ( $Q_{\beta\beta}$ , keV)	$M \cdot t$ , kg·yr	FWHM, keV	BI, c/keV·kg·yr	BI-FWHM, c/kg·yr	$T_{1/2}$ , yr (90% C.L.)	$\langle m_\nu \rangle$ , meV	Experiment, Detector
$^{76}\text{Ge}$ (2039.0)	127.2 (110.7)	2.6–4.9	$5.2 \times 10^{-4}$	$\sim 1.8 \times 10^{-3}$	$> 1.8 \times 10^{26}$	$< 79\text{--}180$	GERDA [27], HPGe Majorana [25], HPGe
	73.3 (64.5)	2.52	$6.6 \times 10^{-3}$	$16.6 \times 10^{-3}$ <sup>(a)</sup>	$> 8.3 \times 10^{25}$	$< 113\text{--}269$	
$^{136}\text{Xe}$ (2457.8)	$\sim 34,000$ <sup>(b)</sup> (970)	$\sim 247$	$\sim 2 \times 10^{-6}$ ( $\sim 7 \times 10^{-5}$ )	$\sim 5 \times 10^{-4}$ ( $\sim 1.7 \times 10^{-2}$ )	$> 2.3 \times 10^{26}$	$< 36\text{--}156$	KamLAND-Zen [24], Xe in liquid scintillator
	290.4 (234.1)	66.4	$1.8 \times 10^{-3}$	0.12	$> 3.5 \times 10^{25}$	$< 93\text{--}286$	

**Table 1.** *Cont.*

Nucleus ( $Q_{\beta\beta}$ , keV)	$M \cdot t$ , kg · yr	FWHM, keV	BI, c/keV · kg · yr	BI · FWHM, c/kg · yr	$T_{1/2}$ , yr (90% C.L.)	$\langle m_\nu \rangle$ , meV	Experiment, Detector
$^{130}\text{Te}$ (2527.5)	1038.4 (288.8)	7.8	$1.5 \times 10^{-2}$	0.12	$>2.2 \times 10^{25}$	$<90\text{--}305$	CUORE [29], LTB $\text{TeO}_2$
$^{128}\text{Te}$ (866.7)	309.33 (78.56)	4.3	1.4	6.0	$>3.6 \times 10^{24}$	-	CUORE [30], LTB $\text{TeO}_2$
$^{82}\text{Se}$ (2997.9)	9.94 (5.29)	20	$3.5 \times 10^{-3}$	$7 \times 10^{-2}$	$>4.6 \times 10^{24}$	$<263\text{--}545$	CUPID-0 [31], LTB $\text{ZnSe}$
	5.90 (4.90)	~250	$\sim 4 \times 10^{-3}$	~1	$>2.5 \times 10^{23}$	$<1200\text{--}3000$	NEMO-3 [26], tracking detector
$^{100}\text{Mo}$ (3 034.4)	2.71 (1.47)	7.4	$4.7 \times 10^{-3}$	$3.5 \times 10^{-2}$	$>1.8 \times 10^{24}$	$<280\text{--}490$	CUPID- Mo [32], LTB $\text{Li}_2\text{MoO}_4$
$^{116}\text{Cd}$ (2813.5)	4.68 (1.22)	170	0.15	25	$>2.2 \times 10^{23}$	$<1000\text{--}1700$	AURORA [37], $\text{CdWO}_4$ scintillator
$^{48}\text{Ca}$ (4268.0)	~108 (~0.12)	241	$10^{-3}$	0.24	$>5.6 \times 10^{22}$ (c)	$<2900\text{--}16,000$	CANDLES-III [23], $\text{CaF}_2$ scintillation crystals

## 2.2. Results for $2\nu\beta\beta$ Decay

In the  $2\nu\beta\beta$  decay process, the nucleus ( $A, Z$ ) is transformed into the nucleus ( $A, Z + 2$ ) with the simultaneous emission of two electrons and two antineutrinos:

$$(A, Z) \rightarrow (A, Z + 2) + 2e^- + 2\bar{\nu}. \quad (3)$$

In this case, the decay probability is written as follows [19,21]:

$$[T_{1/2}(2\nu)]^{-1} = G_{2\nu} g_A^4 | M_{2\nu} |^2, \quad (4)$$

where  $G_{2\nu}$  is the phase space factor (which is accurately known [21,22]),  $| M_{2\nu} |^2$  is the nuclear matrix element, and  $g_A$  is the axial-vector coupling constant. (Usually, the value  $g_A = 1.27$  is used (the free neutron decay value). Currently, however, there is a discussion about a possible decrease of this value in nuclear matter, about the so-called “quenching” (see, for example, discussions in [20,38–40]). The introduction of “quenching” was due to the fact that the calculated NME values in the framework of existing models for ordinary beta decay and  $2\nu\beta\beta$  decay do not coincide with the measured ones. The introduction of quenching just allows the reconciliation of the calculations with the measurements. However, this issue is still not clear and requires further study. In [40], for example, within the framework of the *ab initio* approach, it was demonstrated that no quenching is required, and the whole problem is reduced precisely to the incorrect calculation of the NME.)

This process is of the second order in terms of weak interaction and is not forbidden by any conservation laws. The study of this decay makes it possible to directly measure NME( $2\nu$ ), which also provides important information for NME( $0\nu$ ) calculations. For 11 nuclei,  $2\nu\beta\beta$  decay has already been registered, and the study of this process continues. At present, the accuracy of measuring  $T_{1/2}$  has improved significantly. If the first measurements of this process had an accuracy of  $\sim 10\text{--}40\%$  and were often of a qualitative nature, then in modern experiments, the accuracy of measurements reaches  $\sim 2\%$ . In particle-track experiments (such as NEMO-3), in addition to the total spectrum, the spectra of individual electrons and the angular distributions of electrons are recorded. Table 2 presents the results of the study of  $2\nu\beta\beta$  decay obtained since 2018. It should be noted that most of the measurements were performed with good statistical accuracy and a high value of the signal-to-background ratio. As a result, the  $T_{1/2}$  value for  $^{82}\text{Se}$ ,  $^{100}\text{Mo}$ ,  $^{116}\text{Cd}$ ,  $^{130}\text{Te}$ , and  $^{136}\text{Xe}$  was measured with good accuracy. The most accurate measurements ( $\sim 1.5\text{--}2.5\%$ )

were obtained with low-temperature bolometers ( $^{82}\text{Se}$  [41],  $^{100}\text{Mo}$  [42], and  $^{130}\text{Te}$  [43]). This is due to the fact that such detectors have almost 100% efficiency in the detection of  $2\nu\beta\beta$  events and a well-defined sensitive volume and, as a rule, have a low level of background. The study of the spectra of single electrons in the NEMO-3 experiment with  $^{100}\text{Mo}$  [44] and  $^{82}\text{Se}$  [26] made it possible to establish the dominance of the single-state dominance (SSD) mechanism [45] for transitions in these nuclei. The conclusion about the dominance of the SSD mechanism in  $^{82}\text{Se}$  was also drawn from the analysis of the spectrum of two electrons in [41]. The result for  $^{96}\text{Zr}$  was obtained in a geochemical experiment. The obtained value agrees well with the results obtained in the NEMO-2 and NEMO-3 counter experiments (mean value is  $T_{1/2} = (2.3 \pm 0.2) \times 10^{19}$  years [13]). At the same time, this result is in poor agreement with previous geochemical experiments ( $T_{1/2} = (3.9 \pm 0.9) \times 10^{19}$  years [46] and  $T_{1/2} = (0.94 \pm 0.32) \times 10^{19}$  years [47]), which, however, is not unusual for geochemical measurements.

A precise study of the shape of the spectrum in  $2\nu\beta\beta$  decay is becoming increasingly important in connection with the search for processes outside the framework of the standard model. The main idea is to accurately measure the shape of the spectrum and compare it with the theoretical curve. Deviations from the theoretical shape of the spectrum (taking into account all possible statistical and systematic errors) can be caused by the contribution from processes outside the standard model. This method was used to search for processes with majoron emission (see Section 2.3), bosonic neutrinos [44], and violations of Lorentz invariance [44,48] (see, in addition, recent review [49]). This raises the question of the accuracy of theoretical calculations, i.e., with what accuracy can one calculate the total shape of the spectrum of two electrons, the shape of the spectrum of individual electrons, and their angular distributions. *A priori*, this is not clear. One can only make a cautious assumption that this accuracy is  $\leq 1\%$ . This is indicated by remarks made in [50] that the approximations in the fundamental formulas lead to inaccuracies at the level of less than 1%. The same is evidenced by the experimental data with  $^{100}\text{Mo}$  in the NEMO-3 experiment [44]. In this experiment, 500,000 useful events were registered with an almost zero background (the signal-to-background ratio is  $\sim 80$ ). In this case, the experimental data are in good agreement with the calculated curve (the deviation of the experimental points from the calculated curve does not exceed 1% in almost the entire energy range).

An interesting situation has arisen with the measurement of the  $2\nu\text{KK}$  capture (process with the capture of two electrons from the K shell) in  $^{124}\text{Xe}$ . In 2018, the limit  $T_{1/2} > 2.1 \times 10^{22}$  years (90% C.L.) was obtained in the XMASS-I experiment [51]. Then in 2019, the XENON1T collaboration claimed the observation of this process with  $T_{1/2} = [1.8 \pm 0.5(\text{stat}) \pm 0.1(\text{syst})] \times 10^{22}$  yr [52], which, after accounting for the errors, does not contradict the result published in [51]. In 2022, in the XENON1T experiment with better statistics and new processing, a new value for the  $2\nu\text{ECEC}$  process was obtained,  $T_{1/2} = [1.1 \pm 0.2(\text{stat}) \pm 0.1(\text{syst})] \times 10^{22}$  yr [53], which, at first glance, no longer agrees with the result of [51]. However if we take into account that, for the  $2\nu\text{2K}$  process, the result is transformed into  $T_{1/2}(2\nu\text{KK}) = [1.5 \pm 0.3(\text{stat}) \pm 0.1(\text{syst})] \times 10^{22}$  yr [53], then the contradiction is only at the level of  $\sim 2\sigma$ . In any case, new, independent measurements of this process are needed.

**Table 2.** Results of experiments on the study of  $2\nu\beta\beta$  beta decay (transitions to the ground state of the daughter nucleus) and  $2\nu$ ECEC from 2018 to April 2023. N is the number of useful events; S/B is the signal-to-background ratio. <sup>(1)</sup> For  $2\nu$ ECEC capture.

Nucleus ( $Q_{\beta\beta}$ , keV)	N	$T_{1/2}$ , yr	S/B	Experiment Ref., Year
$^{82}\text{Se}$ (2997.9)	3472	$[9.39 \pm 0.17(\text{stat}) \pm 0.58(\text{syst})] \times 10^{19}$	4	NEMO-3 [26], 2018
	~200,000	$[8.60 \pm 0.03(\text{stat})^{+0.19}_{-0.13}(\text{syst})] \times 10^{19}$	10	CUPID-0 [41], 2019
$^{96}\text{Zr}$ (3356.1)	Geochemical measurement	$2.03^{+0.46}_{-0.31} \times 10^{19}$	-	[54], 2018
$^{100}\text{Mo}$ (3034.4)	500,000	$[6.81 \pm 0.01(\text{stat})^{+0.38}_{-0.40}(\text{syst})] \times 10^{18}$	80	NEMO-3 [44], 2019
	35,638	$[7.12^{+0.18}_{-0.14}(\text{stat}) \pm 0.10(\text{syst})] \times 10^{18}$	10	CUPID-Mo [42], 2020
$^{116}\text{Cd}$ (2813.5)	93,000	$2.63^{+0.11}_{-0.12} \times 10^{19}$	~1.5	AURORA [37], 2018
$^{130}\text{Te}$ (2527.5)	~200,000	$[7.71^{+0.08}_{-0.06}(\text{stat})^{+0.12}_{-0.15}(\text{syst})] \times 10^{20}$	> 1	CUORE [43], 2021
	~90,000	$[2.23 \pm 0.03(\text{stat}) \pm 0.07(\text{syst})] \times 10^{21}$	~30	KamLAND-Zen [55], 2019
$^{136}\text{Xe}$ (2457.8)	~17,468	$[2.27 \pm 0.03(\text{stat}) \pm 0.10(\text{syst})] \times 10^{21}$	> 1	PandaX-4T [56], 2022
	291	$[2.34^{+0.80}_{-0.46}(\text{stat})^{+0.30}_{-0.17}(\text{syst})] \times 10^{21}$	~1	NEXT [57], 2022
$^{124}\text{Xe}$ (2857) <sup>(1)</sup>	-(2 $\nu$ KK)	$> 2.1 \times 10^{22}$ (90% C.L.)	-	XMASS-I [51], 2018
	126 (2 $\nu$ KK)	$[1.8 \pm 0.5(\text{stat}) \pm 0.1(\text{syst})] \times 10^{22}$	~0.2	XENON1T [52], 2019
	262 (2 $\nu$ ECEC)	$[1.1 \pm 0.2(\text{stat}) \pm 0.1(\text{syst})] \times 10^{22}$	~0.2	XENON1T [53], 2022

### 2.3. Search Results for $\beta\beta$ Processes with the Emission of Majoron and Majoron-like Particles

This is a process in which the nucleus ( $A, Z$ ) is transformed into the nucleus ( $A, Z + 2$ ) with the simultaneous emission of two electrons and a majoron (two majorons):

$$(A, Z) \rightarrow (A, Z + 2) + 2e^- + \chi^0 (+\chi^0). \quad (5)$$

In this case, the decay probability is written as follows [21,58]:

$$[T_{1/2}(0\nu\chi^0)]^{-1} = G_{0\nu\chi^0} g_A^4 \langle g_{ee} \rangle^2 |M_{0\nu}|^2, \quad (6)$$

where  $G_{0\nu\chi^0}$  is the phase space factor (which is accurately known [58]),  $|M_{0\nu}|^2$  is the nuclear matrix element,  $g_A$  is the axial-vector coupling constant, and  $\langle g_{ee} \rangle$  is the coupling constant of the majoron to the neutrino (in the case of decay with two majorons, it will be  $\langle g_{ee} \rangle^4$  instead of  $\langle g_{ee} \rangle^2$  in Formula (6)).

Majoron was introduced into theory in the early 1980s as a massless Goldstone boson that appears when the global  $B-L$  symmetry is broken [59]. This majoron is bound to a neutrino and results in double beta decay with the emission of a majoron. The majoron, if it exists, could play an important role in cosmology and astrophysics. In the early 1980s, singlet [60], doublet [61], and triplet [62] models of majoron were proposed. However, the last two models were rejected by the results of precise determination of the Z boson decay width (corresponding to a contribution of  $2.994 \pm 0.012$  neutrinos [63]), since they must add 0.5 or 2 to this value. Later, new theoretical schemes were invented that do not conflict with the width of the Z boson and that lead to the emission of one or two majorons [64–68]. Recently, schemes with massive majoron (or majoron-like particles), which could play the role of dark matter, have become popular [69–72]. Thus, at present, the term “majoron” is used in a broader sense—now it is not only a massless Goldstone boson, but also other (including massive) light scalar and even vector particles [73]. In experiments to search for neutrinoless double beta decay, the classification of decays with the emission of majoron from [74] is usually used. To describe the shape of the spectrum, the spectral index  $n$  is used from the expression for the corresponding phase space volume  $G \sim (Q_{\beta\beta} - T)^n$ , where  $T$  is the kinetic energy of two electrons. Additionally,  $n$  has the values 1, 2, 3, and 7. The corresponding spectra for  $^{100}\text{Mo}$  (as example) are shown in Figure 2. These four

spectra do not cover all possible spectra, but give an idea of the sensitivity of experiments to different types of majoron. Table 3 shows the limits on classic majoron ( $n = 1$ ) obtained in experiments over the past 5 years. Limits on  $\langle g_{ee} \rangle$  are also given (as indicated by the authors of the relevant papers). The most stringent limitation on the coupling constant of majoron with neutrinos was obtained in the EXO-200 experiment,  $\langle g_{ee} \rangle < (0.4 - 0.9) \times 10^{-5}$  at 90% C.L. [75]. Table 4 presents the resulting constraints for the majoron with the spectral index  $n = 2, 3$ , and  $7$ . We emphasize that practically all limits presented in Tables 3 and 4 are the best for corresponding nuclei and transitions. An exception is the limit for the classical majoron ( $n = 1$ ) for  $^{116}\text{Cd}$ . In this case, a slightly better limit was obtained in [76].

**Table 3.** Results of the search for neutrinoless double beta decay with the emission of majoron (spectral index  $n = 1$ ), obtained from 2018 to April 2023.

Nucleus	$Q_{\beta\beta}$ , keV	$T_{1/2}$ , yr (90% C.L.)	$\langle g_{ee} \rangle$ (90% C.L.)	Experiment Ref., Year
$^{76}\text{Ge}$	2039.0	$>6.4 \times 10^{23}$	$<(1.8-4.4) \times 10^{-5}$	GERDA [77] 2022
$^{82}\text{Se}$	2997.9	$>3.7 \times 10^{22}$ $>1.2 \times 10^{23}$	$<(3.2-8.0) \times 10^{-5}$ $<(1.8-4.4) \times 10^{-5}$	NEMO-3 [26] 2018 CUPID-0 [78] 2023
$^{116}\text{Cd}$	2813.5	$>8.2 \times 10^{21}$	$<(6.1-9.3) \times 10^{-5}$	AURORA [37] 2018
$^{136}\text{Xe}$	2457.8	$>4.3 \times 10^{24}$	$<(0.4-0.9) \times 10^{-5}$	EXO-200 [75] 2021

**Table 4.** Results of the search for neutrinoless double beta decay with the majoron emission for the spectral index  $n = 2, 3$ , and  $7$  (obtained from 2018 to April 2023). In case of  $n = 3$ , this is limit for one and two majoron emission modes. In case of  $n = 7$ , limit is for two majoron emission modes. All limits are presented at 90% C.L.

Spectral Index	$^{76}\text{Ge}$ [77]	$^{82}\text{Se}$ [78]	$^{100}\text{Mo}$ [44]	$^{116}\text{Cd}$ [37]	$^{136}\text{Xe}$ [75]
$n = 2$	$>2.9 \times 10^{23}$	$>3.8 \times 10^{22}$	$>9.9 \times 10^{21}$	$>4.1 \times 10^{21}$	$>1.5 \times 10^{24}$
$n = 3$	$>1.2 \times 10^{23}$	$>1.4 \times 10^{22}$	$>4.4 \times 10^{21}$	$>2.6 \times 10^{21}$	$>6.3 \times 10^{23}$
$n = 7$	$>1.0 \times 10^{23}$	$>2.2 \times 10^{21}$	$>1.1 \times 10^{21}$	$>0.89 \times 10^{21}$	$>5.1 \times 10^{22}$

#### 2.4. Results for $\beta\beta$ Transitions to Excited States of Daughter Nuclei

Over the past 5 years, very interesting results have been obtained for such transitions. Tables 5 and 6 show the results for transitions to the first  $2_1^+$  and first  $0_1^+$  states. Results are shown for both  $2\nu\beta\beta$  and  $0\nu\beta\beta$  decays. Transitions to the  $2_1^+$  level are suppressed due to different quantum numbers of the initial and final nuclei. Of greatest interest is the decay into a  $0_1^+$  excited state. In the experiments of the last 5 years, the values of  $T_{1/2}$  for  $^{100}\text{Mo}$  [79] and  $^{150}\text{Nd}$  [80,81] were again measured for  $2\nu\beta\beta$  decay into the  $0_1^+$  excited state. The obtained values agree with the results of previous measurements [13]. Practically all limits presented in Tables 5 and 6 are the best for corresponding nuclei and transitions. An exception is for the limits for the  $2\nu$  transitions in  $^{116}\text{Cd}$ . In these cases, the best limits were obtained in [82].

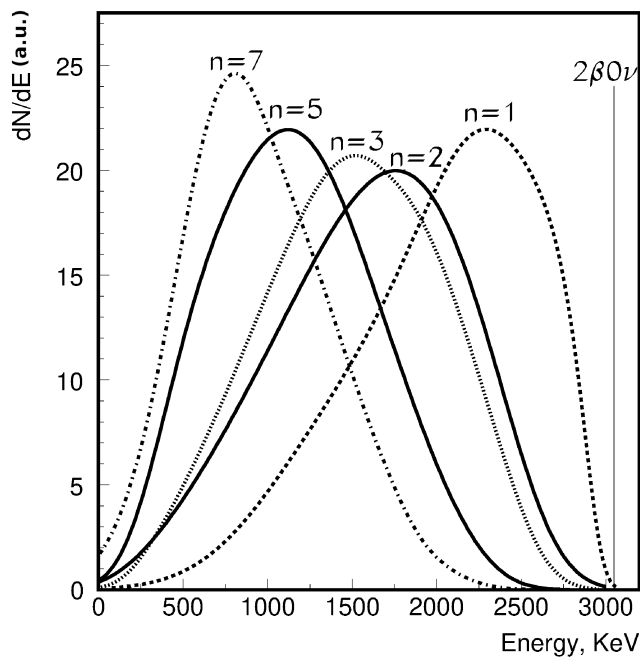


**Figure 2.** Energy spectra of different  $^{100}\text{Mo}$  decay modes:  $2\nu\beta\beta$  ( $n = 5$ ),  $0\nu\chi^0\beta\beta$  ( $n = 1, 2$ , and  $3$ ) and  $0\nu\chi^0\chi^0\beta\beta$  ( $n = 3$  and  $7$ ).  $Q_{\beta\beta}$  for  $^{100}\text{Mo}$  is 3034.4 keV.

**Table 5.** Results of experiments to search for  $\beta\beta$  decay into a  $2_1^+$  excited state of the daughter nucleus for both  $2\nu\beta\beta$  and  $0\nu\beta\beta$  decays (obtained from 2018 to April 2023).  $E_{\beta\beta}$  is energy of transition to  $2_1^+$  excited state.

Nucleus, Ref.	$E_{\beta\beta}$ , keV	$T_{1/2}$ , yr (90% C.L.)	
		$2\nu$	$0\nu$
$^{76}\text{Ge}$ [83]	1479.9	$>7.7 \times 10^{23}$	$>2.12 \times 10^{24}$
$^{82}\text{Se}$ [31]	2221.4	-	$>3.0 \times 10^{23}$
$^{100}\text{Mo}$ [79]	2494.9	$>4.4 \times 10^{21}$	$>2.1 \times 10^{23}$
$^{116}\text{Cd}$ [37]	1519.9	$>9.8 \times 10^{20}$	$>7.1 \times 10^{22}$
$^{150}\text{Nd}$ [80]	3037.4	$>2.4 \times 10^{20}$	$>1.26 \times 10^{22}$

**Table 6.** Results of experiments to search for  $\beta\beta$  decay into the  $0_1^+$  excited state of the daughter nucleus for  $2\nu\beta\beta$  and  $0\nu\beta\beta$  decays (obtained from 2018 to April 2023).  $E_{\beta\beta}$  is energy of transition to  $0_1^+$  excited state.

Nucleus, Ref.	$E_{\beta\beta}$ , keV	$T_{1/2}$ , yr (90% C.L.)	
		$2\nu$	$0\nu$
$^{76}\text{Ge}$ [83]	916.7	$>7.5 \times 10^{23}$	$>3.4 \times 10^{24}$
$^{82}\text{Se}$ [84]	1510.3	$>1.3 \times 10^{21}$	$>2.3 \times 10^{22}$
$^{82}\text{Se}$ [31]	-	-	$>1.8 \times 10^{23}$
$^{100}\text{Mo}$ [79]	1904.1	$[7.5 \pm 0.8(\text{stat})^{+0.4}_{-0.3}(\text{syst})] \times 10^{20}$	$>1.2 \times 10^{23}$
$^{116}\text{Cd}$ [37]	1056.6	$>5.9 \times 10^{20}$	$>4.5 \times 10^{22}$
$^{130}\text{Te}$ [85]	734.0	$>2.5 \times 10^{23}$	$>1.4 \times 10^{24}$
$^{136}\text{Xe}$ [86]	878.8	$>1.4 \times 10^{24}$	-
$^{150}\text{Nd}$ [81]	2630.9	$[0.97^{+0.29}_{-0.19}(\text{stat}) \pm 0.15(\text{syst})] \times 10^{20}$	-
$^{150}\text{Nd}$ [80]	-	$[1.11^{+0.19}_{-0.14}(\text{stat})^{+0.17}_{-0.15}(\text{syst})] \times 10^{20}$	$>1.36 \times 10^{22}$

### 3. Prospects for New Experiments

Table 7 shows the parameters of the most promising future experiments. The main goal of the upcoming experiments is to test the scheme with the inverted ordering of neutrino masses, i.e., to achieve sensitivity to  $\langle m_\nu \rangle \sim 15\text{--}50$  meV. Almost all of the experiments listed in the table will be able to test the inverted hierarchy region. However, the best sensitivity is planned in the CUPID, LEGEND-1000, and nEXO experiments, and it is these experiments that have the greatest chance of detecting  $0\nu\beta\beta$  decay if the inverted ordering of neutrino masses is realized in nature. These experiments are currently under preparation. Apparently, it will take at least 5 years to start the experiments, and another  $\sim 5\text{--}10$  years to take data. Thus, the final results in these experiments will be obtained in  $\sim 10\text{--}15$  years. Let us pay attention to the fact that the LEGEND-200 experiment started a dataset in 2023. The successful implementation of this experiment will serve as a good start for LEGEND-1000. Here, it should be noted that in the case of a normal ordering of neutrino masses, the allowed range of values for  $\langle m_\nu \rangle$  is  $< 30$  meV [87]. This means that these future experiments are also sensitive to the normal ordering, although at  $\langle m_\nu \rangle \sim 15\text{--}30$  meV, it will not be possible to distinguish one type of ordering from another. When implementing the above program of experiments, of course, the study of the processes of two-neutrino double beta decay of  $^{76}\text{Ge}$ ,  $^{100}\text{Mo}$ ,  $^{130}\text{Te}$ , and  $^{136}\text{Xe}$  will be continued. In each case, millions of useful events will be registered, which will make it possible to determine with good accuracy the shape of the corresponding spectra and, with high sensitivity, search for processes outside the framework of the standard model (majoron, bosonic neutrinos, Lorentz invariance violation, etc.). Double beta transitions to excited states for these nuclei will also be investigated with very good sensitivity. There is hope for the first time to register the  $2\nu\beta\beta$  decay of  $^{76}\text{Ge}$  and  $^{136}\text{Xe}$  to the  $0_1^+$  level of the daughter nuclei. Of course, in addition to the experiments listed in Table 7, there are several dozen other proposals that are at the R&D stage. Probably some of them will also be implemented. A more or less complete list of such proposals can be found in reviews [18,88]. For detailed information on some of the planned experiments, see also reviews [89–93].

**Table 7.** Future experiments. M is the mass of the investigated isotope. The sensitivities for  $T_{1/2}$  and  $\langle m_\nu \rangle$  are given as presented by the authors of the respective proposals.

Experiment	Nucleus	M, kg	Sensitivity $T_{1/2}$ , yr (90% C.L.)	Sensitivity $\langle m_\nu \rangle$ , meV (90% C.L.)	Status
LEGEND [94]	$^{76}\text{Ge}$	200	$\sim 10^{27}$	$\sim 34\text{--}80$	Current R&D
		1000	$1.7 \times 10^{28}$	8.5–19.4	
CUPID [95–97]	$^{100}\text{Mo}$	250	$1.4 \times 10^{27}$	10–17	R&D
		1000	$9.2 \times 10^{27}$	4.1–6.8	
nEXO [98]	$^{136}\text{Xe}$	5000	$1.35 \times 10^{28}$	4.7–20.3	R&D
KamLAND2-Zen [99]	$^{136}\text{Xe}$	1000	$\sim 2 \times 10^{27}$	$\sim 12\text{--}52$	R&D
AMoRE [100]	$^{100}\text{Mo}$	100	$\sim (5\text{--}8) \times 10^{26}$	$\sim 13\text{--}28$	R&D
SNO+ [101,102]	$^{130}\text{Te}$	$\sim 1300$	$2.1 \times 10^{26}$	37–89	In progress R&D
		$\sim 8000$	$\sim 10^{27}$	$\sim 20\text{--}40$	

### 4. Conclusions

The analysis of the results of the search and study of the processes of double beta decay reported from the beginning of 2018 to April 2023 are presented here. It is clear that, in the last 5 years, great progress has been made both in the search for  $0\nu\beta\beta$  decay and in the study of  $2\nu\beta\beta$  decay. All this allows us to hope for the successful implementation of a new generation of experiments and the achievement of sensitivity to neutrinoless decay at the level  $\langle m_\nu \rangle \sim 10\text{--}20$  meV. This sensitivity should be reached in  $\sim 10\text{--}15$  years.

If the neutrinoless double beta decay is still not observed, then new experiments with masses of the studied isotope of interest of 10 tons or more will be required (see discussions in [16,87,103]).

**Funding:** This research received no external funding.

**Data Availability Statement:** Not applicable.

**Conflicts of Interest:** The author declares no conflict of interest.

## References

1. Fukugita, M.; Yanagida, T. Baryogenesis without Grand Unification. *Phys. Lett. B* **1986**, *174*, 45–47. [\[CrossRef\]](#)
2. Majorana, E. Teoria simmetrica dell'elettrone e del positrone. *Nuovo Cim.* **1937**, *14*, 171–184. [\[CrossRef\]](#)
3. Pascoli, S.; Petcov, S.T.; Schwetz, T. The absolute neutrino mass scale, neutrino mass spectrum, Majorana CP-violation and neutrinoless double-beta decay. *Nucl. Phys. B* **2006**, *734*, 24–49. [\[CrossRef\]](#)
4. Bilenky, S.M.; Giunti, G. Neutrinoless double-beta decay: A probe of physics beyond the Standard Model. *Int. J. Mod. Phys. A* **2015**, *30*, 1530001. [\[CrossRef\]](#)
5. Vergados, J.D.; Ejiri, H.; Simkovic, F. Neutrinoless double beta decay and neutrino mass. *Int. J. Mod. Phys. E* **2016**, *25*, 1630007. [\[CrossRef\]](#)
6. Girardi, I.; Petcov, S.T.; Titov, A.V. Predictions for the Majorana CP violation phases in the neutrino mixing matrix and neutrinoless double beta decay. *Nucl. Phys. B* **2016**, *911*, 754–804. [\[CrossRef\]](#)
7. Barabash, A.S.; Dolgov, A.D.; Dvornicky, R.; Simkovic, F.; Smirnov, A.Y. Statistics of neutrinos and the double beta decay. *Nucl. Phys. B* **2007**, *783*, 90–111. [\[CrossRef\]](#)
8. Nitescu, O.; Ghinescu, S.; Stoica, S. Lorentz violation effects in  $2\nu\beta\beta$  decay. *J. Phys. G* **2020**, *47*, 055112. [\[CrossRef\]](#)
9. Ghinescu, S.; Nitescu, O.; Stoica, S. Investigation of the Lorentz invariance violation in two-neutrino double-beta decay. *Phys. Rev. D* **2022**, *105*, 05532. [\[CrossRef\]](#)
10. Deppisch, F.F.; Graf, L.; Rodejohann, W.; Xu, X.-J. Neutrino self-interactions and double beta decay. *Phys. Rev. D* **2020**, *102*, 051701. [\[CrossRef\]](#)
11. Bolton, P.D.; Deppisch, F.F.; Graf, L.; Simkovic, F. Two-neutrino double beta decay with sterile neutrinos. *Phys. Rev. D* **2021**, *103*, 055019. [\[CrossRef\]](#)
12. Deppisch, F.F.; Graf, L.; Simkovic, F. Searching for New Physics in two-neutrino double beta decay. *Phys. Rev. Lett.* **2020**, *125*, 171801. [\[CrossRef\]](#)
13. Barabash, A.S. Precise half-life values for two-neutrino double- $\beta$  decay: 2020 review. *Universe* **2020**, *6*, 159. [\[CrossRef\]](#)
14. Belli, P.; Bernabei, R.; Cappella, F.; Caracciolo, V.; Cerulli, R.; Incicchitti, A.; Merlo, V. Double beta decay to excited states of daughter nuclei. *Universe* **2020**, *6*, 239. [\[CrossRef\]](#)
15. Dolinski, M.J.; Poon, A.W.P.; Rodejohann, W. Neutrinoless double-beta decay: Status and prospects. *Ann. Rev. Part. Sci.* **2019**, *69*, 219–251. [\[CrossRef\]](#)
16. Barabash, A.S. Main features of detectors and isotopes to investigate double beta decay with increased sensitivity. *Int. J. Mod. Phys. A* **2018**, *33*, 1843001. [\[CrossRef\]](#)
17. Belli, P.; Bernabei, R.; Caracciolo, V. Status and Perspectives of  $2e$ ,  $e\beta^+$  and  $2\beta^+$  Decays. *Particles* **2021**, *4*, 241–274. [\[CrossRef\]](#)
18. Agostini, M.; Benato, G.; Detwiler, J.A.; Menendez, J.; Vissani, F. Toward the discovery of matter creation with neutrinoless double-beta decay. *arXiv* **2022**, arXiv:2202.01787.
19. Simkovic, F. Neutrino masses and interactions and neutrino experiments in the laboratory. *Physics-Uspekhi* **2021**, *64*, 1238–1260. [\[CrossRef\]](#)
20. Engel, J.; Menendez, J. Status and future of nuclear matrix elements for neutrinoless double-beta decay: A review. *Rep. Prog. Phys.* **2017**, *80*, 046301. [\[CrossRef\]](#)
21. Kotila, J.; Iachello, F. Phase-space factors for double- $\beta$  decay. *Phys. Rev. C* **2012**, *85*, 034316. [\[CrossRef\]](#)
22. Mirea, M.; Pahomi, T.; Stoica, S. Values of the phase space factor involved in double beta decay. *Rom. Rep. Phys.* **2015**, *67*, 872–889.
23. Ajimura, S.; Chan, W.M.; Ichimura, K.; Ishikawa, T.; Kanagawa, K.; Khai, B.T.; Kishimoto, T.; Kino, H.; Maeda, T.; Matsuoka, K. Low background measurement in CANDLES-III for studying the neutrinoless double beta decay of  $^{48}\text{Ca}$ . *Phys. Rev. D* **2021**, *103*, 092008. [\[CrossRef\]](#)
24. Abe, S.; Asami, S.; Eizuka, M.; Futagi, S.; Gando, A.; Gando, Y.; Gima, T.; Goto, A.; Hachiya, T.; Hata, K.; et al. Search for the Majorana nature of neutrinos in the inverted mass ordering region with KamLAND-Zen. *Phys. Rev. Lett.* **2023**, *130*, 051801. [\[CrossRef\]](#) [\[PubMed\]](#)
25. Arnquist, I.J.; Avignone, F.T., III; Barabash, A.S.; Barton, C.J.; Barton, P.J.; Bhimani, K.H.; Blalock, E.; Bos, B.; Busch, M.; Buuck, M.; et al. Final result of the Majorana Demonstrator's search for neutrinoless double- $\beta$  decay in  $^{76}\text{Ge}$ . *Phys. Rev. Lett.* **2023**, *130*, 062501. [\[CrossRef\]](#)
26. Arnold, R.; Augier, C.; Barabash, A.S.; Basharina-Freshville, A.; Blondel, S.; Blot, S.; Bongrand, M.; Boursette, D.; Brudanin, V.; Bustos, J.; et al. Final results on  $^{82}\text{Se}$  double beta decay to the ground state of  $^{82}\text{Kr}$  from the NEMO-3 experiment. *Eur. Phys. J. C* **2018**, *78*, 821. [\[CrossRef\]](#)
27. Agostini, M.; Araujo, G.R.; Bakalyarov, A.M.; Balata, M.; Barabanov, I.; Baudis, L.; Bauer, C.; Bellotti, E.; Belogurov, S.; Bettini, A.; et al. Final results of GERDA on the search for neutrinoless double- $\beta$  decay. *Phys. Rev. Lett.* **2020**, *125*, 252502. [\[CrossRef\]](#)
28. Anton, G.; Badhrees, I.; Barbeau, P.S.; Beck, D.; Belov, V.; Bhatta, T.; Breidenbach, M.; Brunner, T.; Cao, G.F.; Cen, W.R.; et al. Search for neutrinoless double- $\beta$  decay with the complete EXO-200 dataset. *Phys. Rev. Lett.* **2019**, *123*, 161802. [\[CrossRef\]](#)

29. Adams, D.Q.; Alduino, C.; Alfonso, K.; Avignone, F.T., III; Azzolini, O.; Bari, G.; Bellini, F.; Benato, G.; Beretta, M.; Biassoni, M.; et al. Search for Majorana neutrinos exploiting millikelvin cryogenics with CUORE. *Nature* **2022**, *604*, 53–66.

30. Adams, D.Q.; Alduino, C.; Alfonso, K.; Avignone, F.T., III; Azzolini, O.; Bari, G.; Bellini, F.; Benato, G.; Beretta, M.; Biassoni, M.; et al. New direct limit on neutrinoless double beta decay half-life of  $^{128}\text{Te}$  with CUORE. *Phys. Rev. Lett.* **2022**, *129*, 222501. [\[CrossRef\]](#)

31. Azzolini, O.; Beeman, J.W.; Bellini, F.; Beretta, M.; Biassoni, M.; Brofferio, C.; Bucci, C.; Capelli, S.; Caracciolo, V.; Cardani, L.; et al. Final result on the neutrinoless double beta decay of  $^{82}\text{Se}$  with CUPID-0. *Phys. Rev. Lett.* **2022**, *129*, 111801. [\[CrossRef\]](#) [\[PubMed\]](#)

32. Augier, C.; Barabash, A.S.; Bellini, F.; Benato, G.; Beretta, M.; Bergé, L.; Billard, J.; Borovlev, Y.A.; Cardani, L.; Casali, N.; et al. Final results on the  $0\nu\beta\beta$  decay half-life limit of  $^{100}\text{Mo}$  from the CUPID-Mo experiment. *Eur. Phys. J. C* **2022**, *82*, 1033. [\[CrossRef\]](#)

33. Coraggio, L.; Itaco, N.; De Gregorio, G.; Gargano, A.; Mancino, R.; Pastore, S. Present status of nuclear shell-model calculations of  $0\nu\beta\beta$  decay matrix elements. *Universe* **2020**, *6*, 233. [\[CrossRef\]](#)

34. Brase, C.; Menéndez, J.; Coello Pérez, E.A.; Schwenk, A. Neutrinoless double- $\beta$  decay from an effective field theory for heavy nuclei. *Phys. Rev. C* **2022**, *106*, 034309. [\[CrossRef\]](#)

35. Aghanim, N.; Akrami, Y.; Ashdown, M.; Aumont, J.; Baccigalupi, C.; Ballardini, M.; Banday, A.J.; Barreiro, R.B.; Bartolo, N.; Basak, S.; et al. Planck 2018 results. VI. Cosmological parameters. *Astron. Astrophys.* **2020**, *641*, A6.

36. Capozzi, F.; Di Valentino, E.; Lisi, E.; Marrone, A.; Melchiorri, A.; Palazzo, A. Global constraints on absolute neutrino masses and their ordering. *Phys. Rev. D* **2017**, *95*, 096014. [\[CrossRef\]](#)

37. Barabash, A.S.; Belli, P.; Bernabei, R.; Cappella, F.; Caracciolo, V.; Cerulli, R.; Chernyak, D.M.; Danevich, F.A.; d’Angelo, S.; Incicchitti, A.; et al. Final results of the Aurora experiment to study  $2\beta$  decay of  $^{116}\text{Cd}$  with enriched  $^{116}\text{CdWO}_4$  crystal scintillators. *Phys. Rev. D* **2018**, *98*, 092007. [\[CrossRef\]](#)

38. Suhonen, J. Impact of the quenching of  $g_A$  on the sensitivity of  $0\nu\beta\beta$  experiments. *Phys. Rev. C* **2017**, *96*, 055501. [\[CrossRef\]](#)

39. Suhonen, J.; Kostensalo, J. Double  $\beta$  decay and the axial strength. *Front. Phys.* **2019**, *7*, 00029. [\[CrossRef\]](#)

40. Gysbers, P.; Hagen, G.; Holt, J.D.; Jansen, G.R.; Morris, T.D.; Navrátil, P.; Papenbrock, T.; Quaglioni, S.; Schwenk, A.; Stroberg, S.R.; et al. Discrepancy between experimental and theoretical  $\beta$ -decay rates resolved from first principles. *Nat. Phys.* **2019**, *15*, 428–431. [\[CrossRef\]](#)

41. Azzolini, O.; Beeman, J.W.; Bellini, F.; Beretta, M.; Biassoni, M.; Brofferio, C.; Bucci, C.; Capelli, S.; Cardani, L.; Carniti, P.; et al. Evidence of single state dominance in the two-neutrino double- $\beta$  decay of  $^{82}\text{Se}$  with CUPID-0. *Phys. Rev. Lett.* **2019**, *123*, 262501. [\[CrossRef\]](#)

42. Armengaud, E.; Augier, C.; Barabash, A.S.; Bellini, F.; Benato, G.; Benoit, A.; Beretta, M.; Beretta, M.; Berge, L.; Billard, J.; Borovlev, Y.A.; et al. Precise measurement of  $2\nu\beta\beta$  decay of  $^{100}\text{Mo}$  with the CUPID-Mo detection technology. *Eur. Phys. J. C* **2020**, *80*, 674. [\[CrossRef\]](#)

43. Adams, D.Q.; Alduino, C.; Alfonso, K.; Avignone, F.T., III; Azzolini, O.; Bari, G.; Bellini, F.; Benato, G.; Biassoni, M.; Branca A.; et al. Measurement of the  $2\nu\beta\beta$  decay half-life of  $^{130}\text{Te}$  with CUORE. *Phys. Rev. Lett.* **2021**, *126*, 171801. [\[CrossRef\]](#)

44. Arnold, R.; Augier, C.; Barabash, A.S.; Basharina-Freshville, A.; Blondel, S.; Blot, S.; Bongrand, M.; Boursette, D.; Brudanin, V.; Busti, J.; et al. Detailed studies of  $^{100}\text{Mo}$  two-neutrino double beta decay in NEMO-3. *Eur. Phys. J. C* **2019**, *79*, 440. [\[CrossRef\]](#)

45. Domin, P.; Kovalenko, S.; Šimkovic, F.; Semenov, S.V. Neutrino accompanied  $\beta^\pm\beta^\pm$ ,  $\beta^+$ /EC and EC/EC processes within single state dominance hypothesis. *Nucl. Phys. A* **2005**, *753*, 337–363. [\[CrossRef\]](#)

46. Kawashima, A.; Takahashi, K.; Masuda, A. Geochemical estimation of the half-life for the double beta decay of  $^{96}\text{Zr}$ . *Phys. Rev. C* **1993**, *47*, R2452–R2456. [\[CrossRef\]](#)

47. Wieser, M.E.; De Laeter, J.R. Evidence of the double  $\beta$  decay of zirconium-96 measured in  $1.8 \times 10^9$  year-old zircons. *Phys. Rev. C* **2001**, *64*, 024308. [\[CrossRef\]](#)

48. Azzolini, O.; Beeman, J.W.; Bellini, F.; Beretta, M.; Biassoni, M.; Brofferio, C.; Bucci, C.; Capelli, S.; Cardani, L.; Carniti, P.; et al. First search for Lorentz violation in double beta decay with scintillating calorimeters. *Phys. Rev. D* **2019**, *100*, 092002. [\[CrossRef\]](#)

49. Bossio, E.; Agostini, M. Probing beyond the standard model physics with double-beta decays. *arXiv* **2023**, arXiv:2304.07198.

50. Doi, M.; Kotani, T.; Takasugi, E. Double beta decay and Majorana neutrino. *Prog. Theor. Phys. Suppl.* **1985**, *83*, 1–175. [\[CrossRef\]](#)

51. Abe, K.; Hiraide, K.; Ichimura, K.; Kishimoto, Y.; Kobayashi, K.; Kobayashi, M.; Moriyama, S.; Nakahata, M.; Norita, T.; Ogawa, H.; et al. Improved search for two-neutrino double electron capture on  $^{124}\text{Xe}$  and  $^{126}\text{Xe}$  using particle identification in XMASS-I. *Prog. Theor. Exp. Phys.* **2018**, *2018*, 053D03.

52. Aprile, E.; Aalbers, J.; Agostini, F.; Alfonsi, M.; Althueser, L.; Amaro, F.D.; Anthony, M.; Antochi, V.C.; Arneodo, F.; Baudis, L.; et al. Observation of two-neutrino double electron capture in  $^{124}\text{Xe}$  with XENON1T. *Nature* **2019**, *568*, 532–535.

53. Aprile, E.; Abe, K.; Agostini, F.; Ahmed Maouloud, S.; Alfonsi, M.; Althueser, L.; Andrieu, B.; Angelino, E.; Angevaare, J.R.; Antochi, V.C.; et al. Double-weak decays of  $^{124}\text{Xe}$  and  $^{136}\text{Xe}$  in the XENON1T and XENONnT experiments. *Phys. Rev. C* **2022**, *106*, 024328. [\[CrossRef\]](#)

54. Mayer, A.J.; Wieser, M.; Alanssari, M.; Frekers, D.; Matthews, W.; Dilling, J.; Thompson, R.I. Isotope abundance measurement of the half-life of the  $\beta\beta$ -decaying nucleus  $^{96}\text{Zr}$  from a 2.68 Gyr zircon sample. *Phys. Rev. C* **2018**, *98*, 024617. [\[CrossRef\]](#)

55. Gando, A.; Gando, Y.; Hachiya, T.; Ha Minh, M.; Hayashida, S.; Honda, Y.; Hosokawa, K.; Ikeda, H.; Inoue, K.; Ishidoshiro, K.; et al. Precision analysis of the  $^{136}\text{Xe}$  two-neutrino  $\beta\beta$  spectrum in KamLAND-Zen and its impact on the quenching of nuclear matrix elements. *Phys. Rev. Lett.* **2019**, *122*, 192501. [\[CrossRef\]](#)

56. Si, L.; Cheng, Z.; Abdukerim, A.; Bo, Z.; Chen, W.; Chen, X.; Chen, Y.; Cheng, C.; Cheng, Y.; Cui, X.; et al. Determination of double beta decay half-life of  $^{136}\text{Xe}$  with the PandaX-4T natural xenon detector. *Research* **2022**, *2022*, 9798721. [\[CrossRef\]](#)

57. Novella, P.; Sorel, M.; Usón, A.; Adams, C.; Almazán, H.; Álvarez, V.; Aparicio, B.; Aranburu, A.I.; Arazi, L.; Arnquist, I.J.; et al. Measurement of the  $^{136}\text{Xe}$  two-neutrino double beta decay half-life via direct background subtraction in NEXT. *Phys. Rev. C* **2022**, *105*, 055501. [\[CrossRef\]](#)

58. Kotila, J.; Barea, J.; Iachello, F. Phase-space factors and half-life predictions for majoron-emitting  $\beta^- \beta^-$  decay. *Phys. Rev. C* **2015**, *91*, 064310; Erratum in *Phys. Rev. C* **2015**, *92*, 029903. [\[CrossRef\]](#)

59. Chikashige, Y.; Mohapatra, R.N.; Peccei, R.D. Spontaneously broken lepton number and cosmological constraints on the neutrino mass spectrum. *Phys. Rev. Lett.* **1980**, *45*, 1926–1929. [\[CrossRef\]](#)

60. Chikashige, Y.; Mohapatra, R.N.; Peccei, R.D. Are there real goldstone bosons associated with broken lepton number? *Phys. Lett. B* **1981**, *98*, 265–268. [\[CrossRef\]](#)

61. Aulakh, C.; Mohapatra, R. Neutrino as the supersymmetric partner of the majoron. *Phys. Lett. B* **1982**, *119*, 136–140. [\[CrossRef\]](#)

62. Gelmini, G.; Roncadelli, M. Left-handed neutrino mass scale and spontaneously broken lepton number. *Phys. Lett. B* **1981**, *99*, 411–415. [\[CrossRef\]](#)

63. Caso, C.; Conforto, G.; Gurtu, A.; Aguilar-Benitez, M.; Amsler, C.; Barnett, R.M.; Burchat, P.R.; Carone, C.D.; Dahl, O.; Doser, M.; et al. The review of particle physics. *Eur. Phys. J. C* **1998**, *3*, 1.

64. Berezhiani, Z.G.; Smirnov, A.Y.; Valle, J.W.F. Observable majoron emission in neutrinoless double beta decay. *Phys. Lett. B* **1992**, *291*, 99–105. [\[CrossRef\]](#)

65. Mohapatra, R.N.; Takasugi, E. Neutrinoless double beta decay with double majoron emission. *Phys. Lett. B* **1988**, *211*, 192–196. [\[CrossRef\]](#)

66. Burgess, C.P.; Cline, J.M. Majorons without Majorana masses and neutrinoless double beta decay. *Phys. Lett. B* **1993**, *298*, 141–148. [\[CrossRef\]](#)

67. Burgess, C.P.; Cline, J.M. A New class of majoron emitting double beta decays. *Phys. Rev. D* **1994**, *49*, 5925–5944. [\[CrossRef\]](#)

68. Bamert, P.; Burgess, C.P.; Mohapatra, R.N. Multi-majoron modes for neutrinoless double beta decay. *Nucl. Phys. B* **1995**, *449*, 25–48. [\[CrossRef\]](#)

69. Berezhinsky, V.; Valle, J.W.F. The keV majoron as a dark matter particle. *Phys. Lett. B* **1993**, *318*, 360–366. [\[CrossRef\]](#)

70. Garcia-Cely, C.; Heeck, J. Neutrino lines from majoron dark matter. *J. High Energy Phys.* **2017**, *05*, 102. [\[CrossRef\]](#)

71. Brune, T.; Päs, H. Massive majorons and constraints on the majoron-neutrino coupling. *Phys. Rev. D* **2019**, *99*, 096005. [\[CrossRef\]](#)

72. Cepedello, R.; Deppisch, F.F.; González, L.; Hati, C.; Hirsch, M. Neutrinoless double- $\beta$  decay with nonstandard majoron emission, *Phys. Rev. Lett.* **2019**, *122*, 181801. [\[CrossRef\]](#) [\[PubMed\]](#)

73. Carone, C.D. Double beta decay with vector majorons. *Phys. Lett. B* **1993**, *308*, 85–88. [\[CrossRef\]](#)

74. Gunther, M.; Hellmig, J.; Heusser, G.; Hirsch, M.; Klapdor-Kleingrothaus, H.V.; Maier, B.; Päs, H.; Petry, F.; Ramachers, Y.; Strecker, H. Bounds on new majoron models from the Heidelberg-Moscow experiment. *Phys. Rev. D* **1996**, *54*, 3641–3644. [\[CrossRef\]](#)

75. Al Kharusi, S.; Anton, G.; Badhrees, I.; Barbeau, P.S.; Beck, D.; Belov, V.; Bhatta, T.; Breidenbach, M.; Brunner, T.; Cao, G.F.; et al. Search for majoron-emitting modes of  $^{136}\text{Xe}$  double beta decay with the complete EXO-200 dataset. *Phys. Rev. D* **2021**, *104*, 112002. [\[CrossRef\]](#)

76. Arnold, R.; Augier, C.; Baker, J.D.; Barabash, A.S.; Basharina-Freshville, A.; Blondel, S.; Blot, S.; Bongrand, M.; Boursette, D.; Brudanin, V.; et al. Measurement of the  $2\nu\beta\beta$  decay half-life and search for the  $0\nu\beta\beta$  decay of  $^{116}\text{Cd}$  with the NEMO-3 detector. *Phys. Rev. D* **2017**, *95*, 012007. [\[CrossRef\]](#)

77. Agostini, M.; Alexander, A.; Araujo, G.; Bakalyarov, A.M.; Balata, M.; Barabanov, I.; Baudis, L.; Bauer, C.; Belogurov, S.; Bettini, A.; et al. Search for exotic physics in double- $\beta$  decays with GERDA Phase II. *J. Cosm. Astrop. Phys.* **2022**, *12*, 012. [\[CrossRef\]](#)

78. Azzolini, O.; Beeman, J.W.; Bellini, F.; Beretta, M.; Biassoni, M.; Brofferio, C.; Bucci, C.; Capelli, S.; Caracciolo, V.; Cardani, L.; et al. Search for majoron-like particles with CUPID-0. *Phys. Rev. D* **2023**, *107*, 032006. [\[CrossRef\]](#)

79. Augier, C.; Barabash, A.S.; Bellini, F.; Benato, G.; Beretta, M.; Bergé, L.; Billard, J.; Borovlev, Y.A.; Cardani, L.; Casali, N.; et al. New measurement of double beta decays of  $^{100}\text{Mo}$  to excited states of  $^{100}\text{Ru}$  with the CUPID-Mo experiment. *Phys. Rev. C* **2023**, *107*, 025503. [\[CrossRef\]](#)

80. Arnold, R.; Augier, C.; Barabash, A.S.; Basharina-Freshville, A.; Blondel, S.; Blot, S.; Bongrand, M.; Boursette, D.; Breier, R.; Brudanin, V.; et al. Measurement of double beta decay of  $^{150}\text{Nd}$  to the  $0_1^+$  state of  $^{150}\text{Sm}$  in NEMO-3. *arXiv* **2022**, arXiv:2203.03356.

81. Polischuk, O.G.; Barabash, A.S.; Belli, P.; Bernabei, R.; Boiko, R.S.; Cappella, F.; Caracciolo, V.; Cerulli, R.; Danevich, F.A.; Di Marco, A.; et al. Double beta decay of  $^{150}\text{Nd}$  to the first  $0^+$  excited level of  $^{150}\text{Sm}$ . *Phys. Scr.* **2021**, *96*, 085302. [\[CrossRef\]](#)

82. Piepke, A.; Beck, M.; Bockholt, J.; Glatting, D.; Heusser, G.; Klapdor-Kleingrothaus, H.V.; Maier, B.; Perty, F.; Schmidt-Rohr, U.; Strecker, H.; et al. Investigation of the  $\beta\beta$  decay of  $^{116}\text{Cd}$  into excited states of  $^{116}\text{Sn}$ . *Nucl. Phys. A* **1994**, *577*, 493–510. [\[CrossRef\]](#)

83. Arnquist, I.J.; Avignone, F.T., III; Barabash, A.S.; Barton, C.J.; Bertrand, F.E.; Blalock, E.; Bos, B.; Busch, M.; Buuck, M.; Caldwell, T.S.; et al. Search for double- $\beta$  decay of  $^{76}\text{Ge}$  to excited states of  $^{76}\text{Se}$  with the Majorana Demonstrator. *Phys. Rev. C* **2021**, *103*, 015501. [\[CrossRef\]](#)

84. Arnold, R.; Augier, C.; Barabash, A.S.; Basharina-Freshville, A.; Blondel, S.; Blot, S.; Bongrand, M.; Boursette, D.; Breier, R.; Brudanin, V.; et al. Search for the double-beta decay of  $^{82}\text{Se}$  to the excited states of  $^{82}\text{Kr}$  with NEMO-3. *Nucl. Phys. A* **2020**, *996*, 121701. [\[CrossRef\]](#)

85. Adams, D.Q.; Alduino, C.; Alfonso, K.; Avignone, F.T., III; Azzolini, O.; Bari, G.; Bellini, F.; Benato, G.; Biassoni, M.; Branca, A.; et al. Search for double-beta decay of  $^{130}\text{Te}$  to the  $0^+$  states of  $^{130}\text{Xe}$  with CUORE. *Eur. Phys. J. C* **2021**, *81*, 567. [\[CrossRef\]](#)

86. Al Kharusi, S.; Anton, G.; Badhrees, I.; Barbeau, P.S.; Beck, D.; Belov, V.; Bhatta, T.; Breidenbach, M.; Brunner, T.; Cao, G.F.; et al. Search for two-neutrino double-beta decay of  $^{136}\text{Xe}$  to the  $0_1^+$  excited state of  $^{136}\text{Ba}$  with the complete EXO-200 dataset. *arXiv* **2023**, arXiv:2303.01103.

87. Barabash, A.S. Possibilities of future double beta decay experiments to investigate inverted and normal ordering region of neutrino mass. *Front. Phys.* **2019**, *6*, 00160. [\[CrossRef\]](#)

88. Adams, C.; Alfonso, K.; Andreoiu, C.; Angelico, E.; Arnquist, I.J.; Asaadi, J.A.A.; Avignone, F.T.; Axani, S.N.; Barabash, A.S.; Barbeau, P.S.; et al. Neutrinoless double beta decay. *arXiv* **2022**, arXiv:2212.11099.

89. Shimizu, I.; Chen, M. Double beta decay experiments with loaded liquid scintillator. *Front. Phys.* **2019**, *7*, 00033. [\[CrossRef\]](#)

90. Gomez-Cadenas, J.J.; Capilla, F.M.; Ferrario, P. High pressure gas xenon TPCs for double beta decay searches. *Front. Phys.* **2019**, *7*, 00051. [\[CrossRef\]](#)

91. Biassoni, M.; Cremonesi, O. Search for neutrinoless double beta decay with thermal detectors. *Prog. Part. Nucl. Phys.* **2020**, *114*, 103803. [\[CrossRef\]](#)

92. D’Andrea, V.; Di Marco, N.; Junker, M.B.; Laubenstein, M.; Macolino, C.; Morella, M.; Salamida, F.; Vignoli, C. Neutrinoless double beta decay with germanium detectors:  $10^{26}$  yr and Beyond. *Universe* **2021**, *7*, 341. [\[CrossRef\]](#)

93. Poda, D. Scintillation in low-temperature particle detectors. *Physics* **2021**, *3*, 473–535. [\[CrossRef\]](#)

94. Abgral, N.; Abt, I.; Agostini, M.; Alexander, A.; Andreoiu, C.; Araujo, G.R.; Avignone, F.T., III; Bae, W.; Bakalyarov, A.; Balata, M.; et al. The large enriched germanium experiment for neutrinoless  $\beta\beta$  decay, LEGEND-1000 preconceptual design report. *arXiv* **2021**, arXiv:2107.11462.

95. Armstrong, W.R.; Chang, C.; Hafidi, K.; Lisovenko, M.; Novosad, V.; Pearson, J.; Polakovic, T.; Wang, G.; Yefremenko, V.; Zhang, J.; et al. CUPID pre-CDR. *arXiv* **2019**, arXiv:1907.09376.

96. Alfonso, K.; Armatol, A.; Augier, C.; Avignone, F.T., III; Azzolini, O.; Balata, M.; Barabash, A.S.; Bari, G.; Barresi, A.; Baudin, D.; et al. CUPID: The next-generation neutrinoless double beta decay experiment. *J. Low Temp. Phys.* **2023**. [\[CrossRef\]](#)

97. Armatol, A.; Augier, C.; Avignone, F.T., III; Azzolini, O.; Balata, M.; Ballen, K.; Barabash, A.S.; Bari, G.; Barresi, A.; Baudin, D.; et al. Toward CUPID-1T. *arXiv* **2022**, arXiv:2203.08386.

98. Adhikari, G.; Al Kharusi, S.; Angelico, E.; Anton, G.; Arnquist, I.J.; Badhrees, I.; Bane, J.; Belov, V.; Bernard, E.P.; Bhatta, T.; et al. nEXO: Neutrinoless double beta decay search beyond  $10^{28}$  year half-life sensitivity. *J. Phys. G* **2022**, *49*, 015104. [\[CrossRef\]](#)

99. Ishimizu, I. Search for Majorana neutrinos. *arXiv* **2023**, arXiv:2303.05127.

100. Oh, Y. Status of AMoRE. *J. Phys. Con. Ser.* **2022**, *2156*, 012146. [\[CrossRef\]](#)

101. Albanese, V.; Alves, R.; Anderson, M.R.; Andringa, S.; Anselmo, L.; Arushanova, E.; Asahi, S.; Askins, M.; Auty, D.J.; Back, A.R.; et al. The SNO+ experiment. *JINST* **2021**, *16*, P08059. [\[CrossRef\]](#)

102. Inacio, A.S. Status and prospects of the SNO+ experiment. *PoS* **2022**, PANIC2021, 274.

103. Barabash, A.S. The new generation of double beta decay experiments: Are there any limitations? *J. Phys. G* **2012**, *39*, 085103. [\[CrossRef\]](#)

**Disclaimer/Publisher’s Note:** The statements, opinions and data contained in all publications are solely those of the individual author(s) and contributor(s) and not of MDPI and/or the editor(s). MDPI and/or the editor(s) disclaim responsibility for any injury to people or property resulting from any ideas, methods, instructions or products referred to in the content.